Stray current vs anodic polarization in reinforced mortar: a comparative study on steel corrosion behaviour in both regimes

Chen, Zhipei; Koleva, Dessi; van Breugel, Klaas

Publication date
2015

Published in
European corrosion congress : Earth, Water, Fire, Air, Corrosion happens everywhere

Citation (APA)
Chen, Z., Koleva, D., & van Breugel, K. (2015). Stray current vs anodic polarization in reinforced mortar: a comparative study on steel corrosion behaviour in both regimes. In *European corrosion congress : Earth, Water, Fire, Air, Corrosion happens everywhere* (pp. 1-10)

Stray current vs anodic polarization in reinforced mortar: a comparative study on steel corrosion behaviour in both regimes

Zhipei Chen[1], Dessi Koleva[1,2], Klaas van Breugel[1]

[1]Delft University of Technology, Faculty of Civil Engineering and Geosciences, Materials and Environment, Stevinweg 1, 2628 CN, Delft, The Netherlands
[2]Curtin University of Technology, Faculty of Science and Engineering, Department of Chemical Engineering, GPO Box U1987, Perth, WA, Australia

Summary

Stray current arising from direct current electrified traction systems and then circulating in reinforced concrete structures may initiate corrosion or even accelerate existing corrosion processes on embedded reinforcement. Therefore, stray-current induced corrosion of nearby reinforced concrete structures deserves more attention in view of maintaining structures‘ integrity. The current state-of-the-art generally reports on simulating stray current corrosion through anodic polarization, rather than stray current effects on the corrosion behaviour of steel in reinforced concrete. This work presents the comparison of effects of stray current (through the application of external DC electrical field) and direct anodic polarization on the corrosion behaviour of steel, embedded in mortar specimens. The level of stray current and anodic polarization were set at 0.3 mA/cm^2 and evolution of electrochemical response over time was monitored via OCP (Open Circuit Potential) and EIS (Electrochemical Impedance Spectroscopy). The steel response was recorded as a result from “under polarization” conditions in both anodic and stray current regimes and compared to “rest” (no polarization) conditions.

1 Introduction

The electrical current drawn by vehicles returns to the traction power substation through the running rails. This, besides forming part of the signalling circuit for the control of train movements, together with return conductors, represents the current return circuit path [1-5]. However, owing to the longitudinal resistance of the rails and their imperfect insulation to ground, part of the return current leaks out from the running rails, i.e. stray current forms, and returns to the traction power substation through the ground and underground metallic structures (such as steel re-bars in concrete) [6, 7]. Stray direct currents (DC) are known to be much more dangerous than stray alternating currents (AC), circulating of which in reinforced concrete structures may initiate corrosion or even accelerate existing corrosion processes on embedded reinforcement [1]. To study the effects of stray current on corrosion behavior of steel in concrete, various works report different aspects. Current state-of-the-art generally reports on anodic polarization, rather than stray current effects on the corrosion behaviour of steel in reinforced specimens [8-10]. Although the effect of stray current is reflected in the generation of anodic locations on a steel surface (i.e. the degradation itself could be linked to anodic currents), the stray current distribution and influence would be more complex. Consequently, research on the different in

nature effects of stray current and anodic polarization on steel corrosion behaviour is necessary and of significant importance.

This work will discuss the effects of stray current (through the application of external DC electrical field) and direct anodic polarization on the corrosion behaviour of steel embedded in mortar specimens. The level of stray current and anodic polarization were set on the level of 0.3 mA/cm^2. The evolution of electrochemical response over time was monitored via OCP (Open Circuit Potential) and EIS (Electrochemical Impedance Spectroscopy). A comparison of response was made as a result of "under polarization" conditions in both anodic and stray current regimes and correlated to "rest" (no polarization) conditions.

2 Experimental

2.1 Materials and Specimen Preparation

The specimens investigated in this work are reinforced mortar prisms of 40×40×160 mm. The specimens were cast from CEM I 42.5 N and normed sand. The Binder/Sand ratio and Water/Binder ratio were 1:3 and 0.5, respectively. The embedded steel was type FeB500HKN (d=6mm), with exposed length of 40 mm. Prior to casting and in view of planned weight loss measurements, the steel rebars were cleaned electrochemically (cathodic treatment with 100 A/m^2 current density, using stainless steel as anode) in solution of 75 g NaOH, 25 g Na_2SO_4, 75 g Na_2CO_3, reagent water to 1000 mL, according to ASTM G-1 [11]. The schematic presentation of the test specimens is depicted in Fig. 1: the two ends of the rebars were covered by heat-shrinkable tube (blue parts in Fig. 1), in order to restrict the exposed surface area.

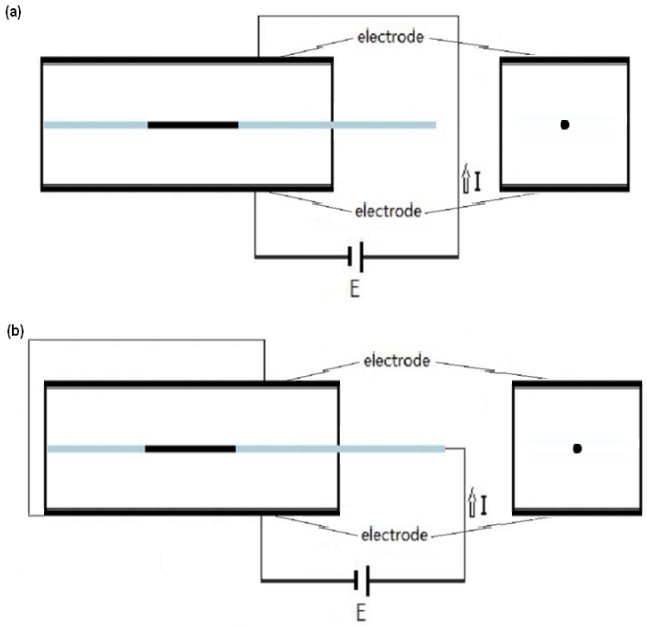

Figure 1: Experimental set-up and position of electrodes: (a) stray current; (b) anodic polarization

For the convenience of comparison between stray current and anodic polarization, the applied levels for both regimes were set to 0.3 mA/cm^2. The experimental set-up and electrodes configuration are as presented in Fig.1. The two Ti electrodes (MMO

Ti mesh, 40×160 mm^2) cast-in within samples preparation served as terminals for polarization and stray current application. When both polarization regimes were interrupted (min 24h before electrochemical tests), the Ti electrodes served as counter electrode in a general 3-electrode set-up, where the re-bar was the working electrode and an external Saturated calomel electrode (SCE) served as a reference electrode.

2.2 Curing Conditions

After casting and prior to demoulding and conditioning, all specimens were cured in fog room (98% RH, 20 ºC) for 24 hours. The specimens were conditioned after demoulding – Table 1. All specimens were immersed with 2/3rd of height in water or 5% NaCl solution.

Table 1: Details conditioning regimes

Group	External environment	Current supply
R	Water (2/3)	--
C	5% NaCl (2/3)	--
S	Water (2/3)	Stray current
A	Water (2/3)	Anodic polarization
CS	5% NaCl (2/3)	Stray current
CA	5% NaCl (2/3)	Anodic polarization

2.3 Testing Methods

The electrochemical measurements were performed at open circuit potential (OCP) for all cells using SCE as reference electrode (as above specified, the counter electrode was the initially embedded MMO Ti). The used equipment was Metrohm Autolab (Potentiostat PGSTAT30), combined with FRA2 module. EIS measurements were performed after 3d, 7d, 14d and 28d of conditioning in the frequency of 50 kHz - 10 mHz, by superimposing an AC voltage of 10mV (rms). A 24h polarization (potential) decay applied before each EIS test. Over the depolarization process and during EIS tests, the specimens were immersed fully in water/5% NaCl solution. The control samples (Group R) was also monitored according to above test procedure.

3 Results and discussion

This paper presents and discusses the first observations and results from a running experiment. The evolution of open circuit potential (OCP) values is discussed as a comparison of all studied regimes, indicating the corrosion state of the steel reinforcement. Electrochemical Impedance spectroscopy (EIS) was performed from the start of the experiment and presented until 28 days of conditioning. EIS is discussed mainly as a qualification of the observed response, whereas quantitative (preliminary) information is presented for 28 days only. Additionally, the manner of fitting the EIS data and relevant considerations are also discussed.

3.1 OCP evolution

Fig. 2 depicts the open circuit potentials evolution with time for all conditions i.e. corroding (Group C, S, A, CS, CA) and reference (Group R) specimens (up to 28 days of age and conditioning respectively). The first measurement was taken 48h after

immersion in the relevant environment, which was 24h conditioning and 24h decay for the “under polarization” specimens. Due to the electrochemical cleaning, prior to casting, and in view of the “fresh” mortar matrix (only 24h fog room curing), the initial open circuit potentials (e.g. 1d) show active state (recorded potential values of -400 to -560 mV vs SCE). This is beyond the threshold of passivity i.e. more cathodic than the generally accepted -200±70 mV vs SCE for reinforced mortar (concrete) systems [12]. Later on, for the control group (R) the OCP values shift as expected to more noble values, reaching -260 mV after two weeks. This indicates stabilisation of the passive layer on the steel surface with time - as expected for medium of pH 12.5 – 13.5. Similar trend of OCP ennoblement was recorded for group S (specimens conditioned in Cl-free environment, subjected to stray current): within 1 week of treatment, the OCP values for group S present even more anodic values, suggesting intensified process of passive layer formation/stabilisation. This would be the result of enhanced water and ion transport in the bulk matrix and interfaces due to stray current flow. Further, the OCP for group S stabilises at more cathodic values, compared to group R, already suggesting a reversed influence of the stray current or, at the very minimum, competing mechanisms of steel activation and passive layer build-up.

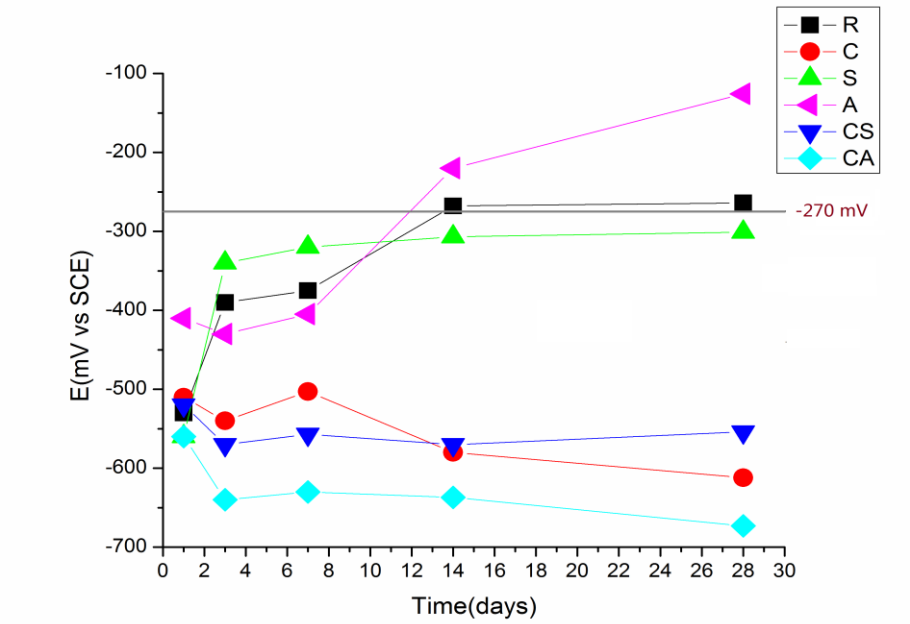

Figure 2: Evolution of open circuit potential with time (R: Reference group; C: Cl^-; S: Stray current; A: Anodic polarization; CS: Cl^- + Stray current; CA: Cl^- + Anodic polarization)

For the specimens in group A – immersed in water with anodic polarization applied, the recorded OCP values present a more distinctively different trend. Initially, the effect of anodic polarisation is immediately recorded by an OCP value (after decay) of around -400 mV, whereas all other specimens exhibited more cathodic values (as already discussed). Well known is that with anodic polarization, in the absence of corrodents (as chloride ions) and in alkaline medium, a product (passive) layer will be forced to form i.e. with constant anodic current the electrode potential will gradually rise towards a stable value. Stability of this layer will be reflected by reaching a value of 600 mV (SCE), which is the potential of oxygen evolution on a passive steel surface in this environment. As seen from Fig.2, the OCP of group S initially fluctuates around -400 mV, followed by a steady and gradual increase towards more anodic values after 1 week of conditioning. At this stage of more than 60 days (not shown in the figure) the OCP for group S is in the range of 400 mV (SCE) and more positive,

therefore polarisation measurements will be performed to evaluate stability of the passive layer and the possibility for already transpassive steel dissolution.
For the cases where chloride is present in the external environment, i.e. groups C, CS and CA, chloride-induced activation is the predominant mechanism, reflected by maintained cathodic potentials from the beginning of the test and within conditioning.
As can be observed, the group C – specimens conditioned in 5%NaCl, exhibit the expected behaviour of initial potential drop and stabilisation of around -600 mV. This potentials are slightly more negative, compared to usually measured such within Cl-induced corrosion in reinforced cement-paste materials (between -450 and -550 mV), the reason being denoted to the “fresh” cement-based bulk matrix i.e. increased relative humidity and still initial stages of cement hydration.
For group CS i.e. chloride-containing external medium and stray current, the OCP evolution follows similar to group C trend. If the response of group CS is compared to group S only, well observed is the effect of chloride ions on corrosion initiation and propagation i.e. a synergy of two detrimental effects. This is well seen in the initial stages, the OCP values for group CS being more cathodic than these for group C. From two week onwards a slight anodic OCP shift was observed, denoted to competing mechanisms of Cl-induced corrosion and possible attempts for re-passivation in alkaline medium with enhanced ion and water transport. The OCP for group CS, however, remains in the active domain.
The most pronounced negative effect of the synergy of polarisation and chloride-induced corrosion is recorded in group CA – specimens conditioned in 5% NaCl with applied anodic polarization. Despite the sustained anodic current here, a stable passive layer cannot form on the steel surface. In Cl-containing alkaline environment, localised corrosion initiation and propagation are taking place with the formation of Cl-containing iron oxides and hydroxides. In addition, the anodic current applied to the steel reinforcement accelerates Cl ions migration towards the steel/cement paste interface, which would be significantly pronounced in the not yet mature cement-based matrix. Therefore, the behaviour of CA specimens ends up significantly different from all other cases.
The qualitative assessment of corrosion state of the embedded steel re-bar in each studied condition as reflected by OCP records is further supported by EIS measurements, which will be discussed in what follows.

3.2 EIS Response

The experimental impedance responses (Nyquist format) for all groups are presented in Figures 3 to 5 as an overlay from 3d to 28d per specimens’ group (specimens geometry and active steel surface is equal, therefore normalization of the plots was not performed). In view of the fact that the experiment is still running and hereby summarized are the first series of results, the EIS response is mainly discussed qualitatively. An example of the employed quantitative characterization and some preliminary results for 28 days response are also presented further below. For groups R and C, the shape of the experimental curves is reflecting the typical response of steel in cement based environment (alkaline medium), without, Fig.3a) and with, Fig.3b), the presence of chloride [13]. Well known and accepted interpretation of this response is that the high frequency (HF) domain and HF to middle frequency (MF) domain reflect the contribution of the cement-based material (including electrolyte resistance, which is negligible in this case), whereas the MF to low frequency (LF) and LF domains reflects the phenomena at the steel/cement paste interface and steel electrochemical

response. For group R the EIS response is almost capacitive (close to straight lines, slightly inclined from the imaginary axis), indicating passive state. This is accompanied by a increased slope of the curves (increasing α-values) in the LF domain, denoted to steel response i.e. to further stabilization of the passive state.

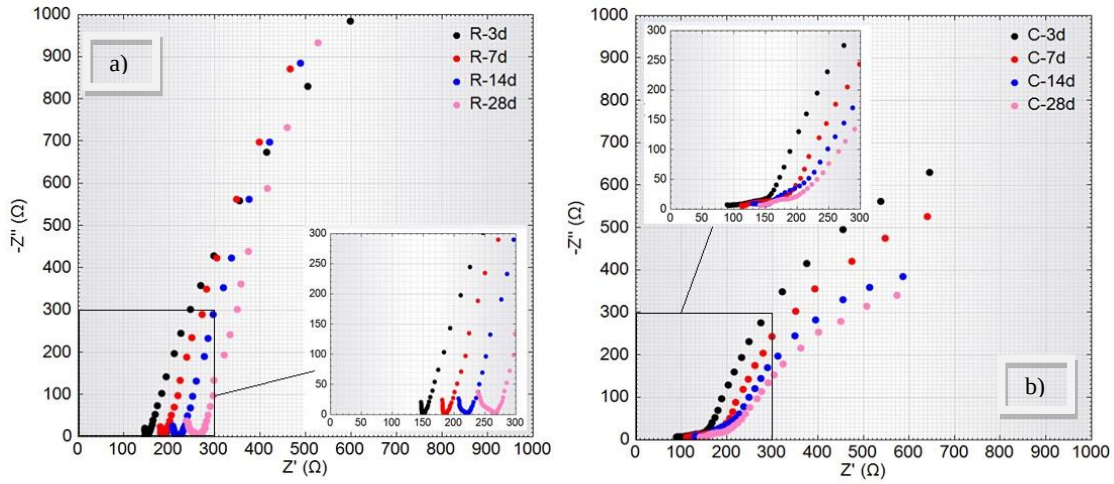

Figure 3: EIS response as an overlay of 3 to 28 days for control group R (a) and corroding group C (b)

In contrast to group R, the EIS responses for group C (specimens immersed in NaCl) show clear evidence of active corrosion on the steel surface. Starting at very early stage (3 days) the response is already an inclined to the real axis semi-circle with a decreasing magnitude of |Z| towards the 28 days. The shape of this EIS response had been largely reported to be due to the presence of chloride ions on the steel surface and increasingly active corrosion state [13]. Fig. 4 similarly presents the EIS response for groups S (stray current, water as external medium) and group A (anodic polarization, water as external medium).

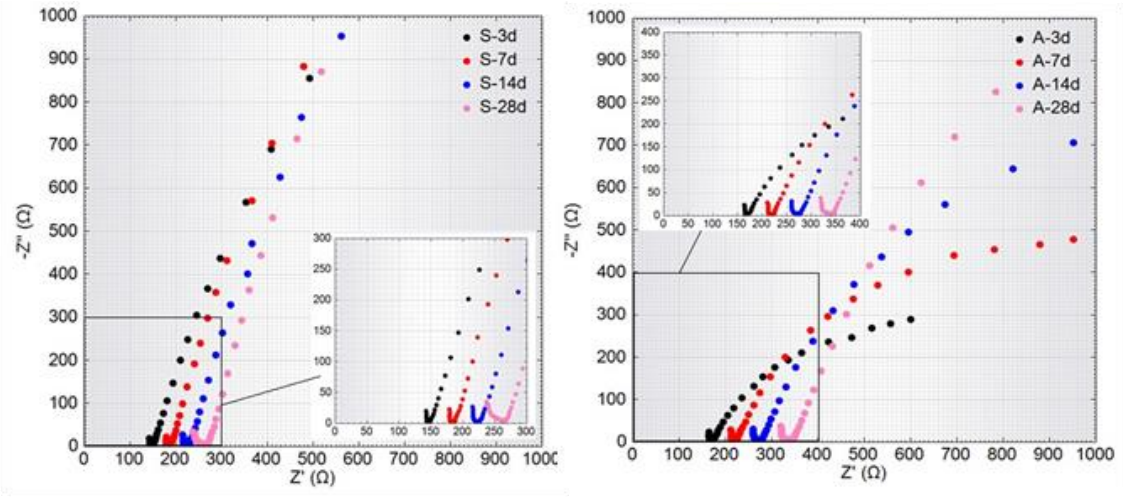

Figure 4: EIS response as an overlay of 3 to 28 days for group S (a) and group A (b)

The response for group S is similar to that for the control group R, except for the less pronounced increase of the slope of the curves towards higher values i.e. impeded compared to group R stabilization of the passive layer. This is well in line with the observed OCP records (Fig.2), where for group S the potential values changed from more noble to more cathodic compared to group R. At a first approximation, the response for group A (Fig.4b) seems to present behavior even more active than group

C (Fig.3b). This behavior is also in line with the cathodic OCP values for group A (Fig.2) within the start of the test (approx. -400 mV) and until 7 days (of course keeping in mind that OCP is an indication of behavior and depends on various factors). From 7 days onwards, however, the EIS response presents an increase of corrosion resistance for group A i.e. inclination of the response towards the imaginary axis and increase of magnitude of |Z|. This is due to the enhanced formation and stabilization of iron oxide/hydroxide layer on the steel surface under the externally applied constant anodic current and is in line with the enablement of OCP values for group A towards 28 days (Fig.2).

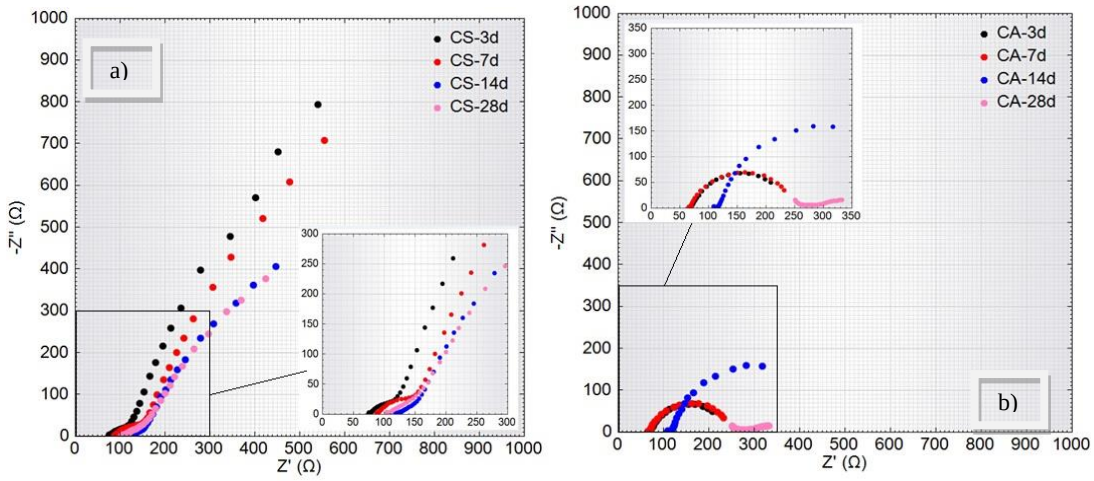

Figure 5: EIS response as an overlay of 3 to 28 days for group CS (a) and group CA (b)

Finally, the response of the “under stray current” and “under anodic polarization” groups, CS and CA respectively, conditioned in NaCl solution are presented in Fig.5. As can be observed, the synergetic action of two degradation factors i.e. polarization and chloride ions in the environment, results in significantly lower corrosion resistance for both cases. For the CS group, a dominant factor is obviously the effect of chloride ions, since the magnitude of |Z| is significantly lower for group CS (Fig.5a), compared to group S (Fig.4a) and similar to group C (Fig.4b). The most active behavior of all discussed cases is obviously in group CA (Fig.5b), presenting a significant drop of impedance over time due to the inability for formation of a more resistance oxide layer (as observed in group A) in the presence of chloride-containing environment. For both CS and CA groups the EIS response is well supported by the recorded cathodic OCP values (Fig.2): in the former case, for CS, slight enablement was recorded at later stages, corresponding to impeded activity as reflected by similar EIS response for 14 and 28 days (Fig.5a) and if compared to the enhanced corrosion propagation for specimens C (Fig.4b) and specimens CA (Fig.5b) at these stages. For the latter case, specimens CA, altered activity was observed, from active and similar response at 3 days and 7 days, through increased magnitude of |Z| at 14 days (due to larger in volume but not protective product layer on the steel surface), to a significantly more active state at the stage of 28 days.

As a conclusion from the above discussion, it can be stated that stray current effects and anodic polarization cannot be considered similarly affecting the corrosion response of steel when stray-current induced corrosion is to be studied. Moreover, the presence of chlorides in the environment significantly contributes to both types of polarization effects and needs to be considered, separately and in a combination of other factors, in order to avoid underestimation or overestimation of corrosion re-

sistance. What also needs to be mentioned is that the specimens in this work were cured for only 24h, therefore all recorded effects are more pronounced if compared to conditions of longer curing. Additionally, longer monitoring period is required in order to more accurately determine all synergetic effects. To this end, the EIS section will conclude with an example of the EIS fitting procedure so far and the (preliminary) derived global polarization values for the embedded steel at the stage of 28 days. Figure 6 depicts the experimental response and fit of a specimen from group C (corroding in NaCl, no polarization) in both Nyquist and Bode plots format. The figure also presents two equivalent circuits, where the 2-time constant one results in a worse fit in the HF domain (inlet in the Bode plot), whereas the second one (3-time constants) results in a very good fit (fitted lines in both plots and inlet in the Nyquist plot).

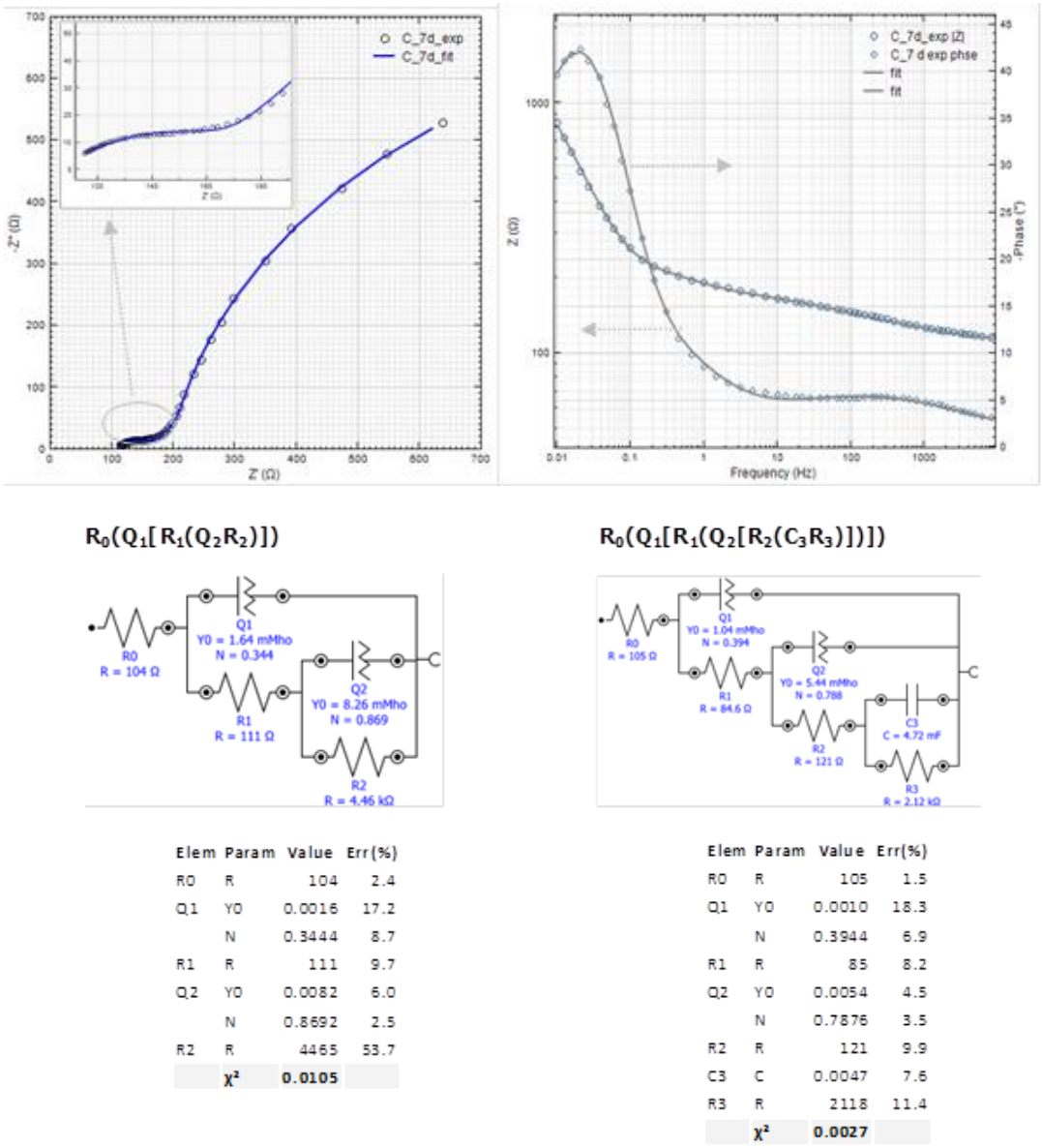

Elem	Param	Value	Err(%)
R0	R	104	2.4
Q1	Y0	0.0016	17.2
	N	0.3444	8.7
R1	R	111	9.7
Q2	Y0	0.0082	6.0
	N	0.8692	2.5
R2	R	4465	53.7
	χ^2	0.0105	

Elem	Param	Value	Err(%)
R0	R	105	1.5
Q1	Y0	0.0010	18.3
	N	0.3944	6.9
R1	R	85	8.2
Q2	Y0	0.0054	4.5
	N	0.7876	3.5
R2	R	121	9.9
C3	C	0.0047	7.6
R3	R	2118	11.4
	χ^2	0.0027	

Figure 6: EIS response and fit for specimen C after 7 days of conditioning and equivalent circuits used (the fit curves and inlet in the Nyquist plot present the result with the 3-time constant circuit; the inlet in the Bode plot – HF with 2-time constant circuit)

For both circuits, R_0 is the resistance of the electrolyte and contribution of the mortar bulk; the first time constant (R_1 and Q_1) is attributed to the pore network of the mortar matrix; the second time constant for the 2-time constant circuit (R_2 and Q_2) deals with

the electrochemical reaction on the steel surface. In the 3-time constant circuit, this last response is actually split between the resistance and pseudo-capacitance of the product layer (R_2 and Q_2) and the charge transfer resistance and double layer capacitance (R_3 and C_3). A circuit with three time constants represents more accurately the actual response as seen in Fig.6, especially with enhanced corrosion activity. Pseudo-capacitance is well known to be used when a non-ideal capacitive behavior is present, whereas the contribution of the bulk cement matrix in this study is restricted because of the starting HF window of 50 kHz only i.e. pore network contribution of connected and disconnected pore space can be claimed rather than properties of the solid matrix. Using similar to the above considerations and calculation procedure, the global polarization resistance of the embedded steel was calculated for all cases (R_p being derived based on R_2 and R_3 parameters). Fig. 7 depicts the normalized R_p values and the C_{dl} values for 28 days of conditioning. As can be observed, the highest corrosion resistance was recorded as expected in the control group R, followed by similar R_p values for group S. The specimens in group A exhibit lower R_p values but accompanied by very low double layer capacitance, denoted to the formation of a more compact product layer on the steel surface.

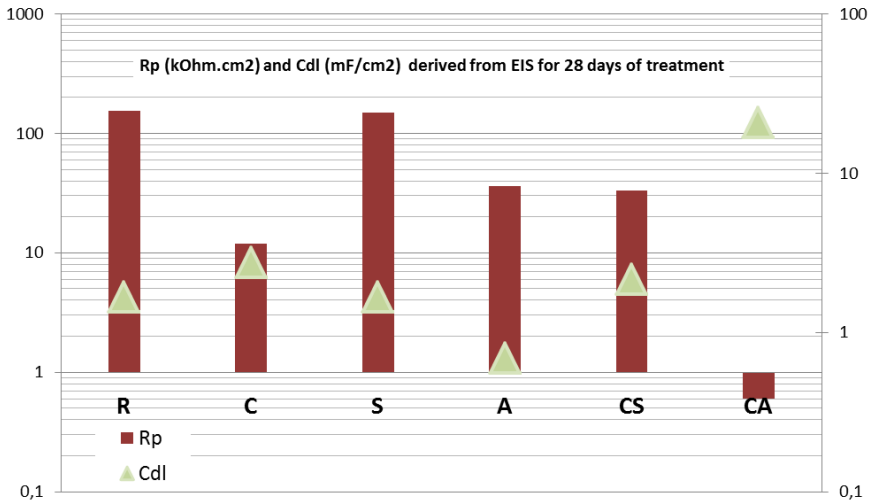

Figure 7: R_p the C_{dl} values for all specimens at the stage of 28 days of conditioning

Comparing specimens C and CS, higher corrosion activity is relevant for specimens C, where lower R_p and higher capacitance values were recorded, due to increasing in volume, non-protective and non-adherent corrosion product layer formation. The lowest corrosion resistance and significantly higher capacitance, denoted to the already discussed most active corrosion state for all studied conditions, are relevant for specimens CA.

4 Conclusions

In this work, a comparitive study was proposed for investigating the different effects of stray current and direct anodic polarization on the corrosion behavior of steel embedded in mortar specimens. At this stage of the running experiment, the following conclusions can be drawn:

1. When it comes to stray current or anodic polarization, relatively positive open circuit potential of steel may be caused by the disturbance of supplied current, which cannot be taken as conclusive evidence of the passive state of the steel. Further

information should be attained from other techniques (EIS response for example) to confirm the actual electrochemical state of steel.
2. Initiation of stray current induced corrosion needs time, and existence of Cl^- can accelerate this process.
3. Anodic polarization with the coexistence of chloride can initiate corrosion much sooner than stray current polarization, and will lead to a more active corrosion comparing to stray current.
4. Consequently, anodic polarization should not be adopted to simulate stray current in practical investigations related to the subject of stray current corrosion.

5 References

[1] L. Bertolini, M. Carsana, P. Pedeferri, Corrosion behaviour of steel in concrete in the presence of stray current, Corrosion Science, 49 (2007) 1056-1068.

[2] I.A. Metwally, H.M. Al-Mandhari, A. Gastli, A. Al-Bimani, Stray currents of ESP well casings, Engineering Analysis with Boundary Elements, 32 (2008) 32-40.

[3] R.W. Revie, Corrosion and corrosion control, John Wiley & Sons2008.

[4] C.L. Wang, C.Y. Ma, Z. Wang, Analysis of stray current in metro DC tractionpower system, Urban Mass Transit, 3 (2007) 51-56.

[5] M. Wu, Progress of the durability of concrete structure of the subway, 1st International Conference on Civil Engineering, Architecture and Building Materials, CEABM 2011Haikou, 2011, pp. 1456-1459.

[6] L. Sandrolini, Analysis of the insulation resistances of a high-speed rail transit system viaduct for the assessment of stray current interference. Part 1: Measurement, Electric Power Systems Research, 103 (2013) 241-247.

[7] Z. Chen, D. Koleva, E. Koenders, K. van Breugel, Stray Current Induced Corrosion Control in Reinforced Concrete by Addition of Carbon Fiber and Silica Fume, MRS Online Proceedings Library, 1768 (2015).

[8] C. Lingvay, A. Cojocaru, T. Vişan, I. Lingvay, Degradations of reinforced concrete structures due to d.c. and a.c. stray currents, UPB Sci Bull Ser B, 73 (2011) 143-152.

[9] H.W. Teng, S.M. Yang, Z.C. Shu, Y. Huang, D. Huo, Simulation experiment of loading influence to reinforcement corrosion affected by stray current and salt solution, Wuhan Ligong Daxue Xuebao, 32 (2010) 147-151.

[10] S.J. Duranceau, W.J. Johnson, R.J. Pfeiffer-Wilder, A Study Examining the Effect of Stray Current on the Integrity of Continuous and Discontinuous Reinforcing Bars, Experimental Techniques, 35 (2011) 53-58.

[11] Standard practice for preparing, cleaning, and evaluating corrosion test specimens, Annual Book of ASTM Standards, (2003) 17-25.

[12] C. Alonso, M. Castellote, C. Andrade, Chloride threshold dependence of pitting potential of reinforcements, Electrochimica Acta, 47 (2002) 3469-3481.

[13] D.A. Koleva, K. van Breugel, J.H.W. de Wit, E. van Westing, N. Boshkov, A.L.A. Fraaij, Electrochemical Behavior, Microstructural Analysis, and Morphological Observations in Reinforced Mortar Subjected to Chloride Ingress, Journal of The Electrochemical Society, 154 (2007) E45.